The Influence of Tempering Time and Temperature on the Structure and Oxidation Behavior of Zr-2.5wt%Nb ☆

*L.V. Ramanathan and I. Costa**

ABSTRACT

The influence of tempering beta-quenched commercial grade Zr-2.5wt%Nb alloy at 500, 550, and 600°C for 10, 100, and 1000 hours on its microstructure and isothermal oxidation behavior at 600°C in oxygen has been investigated. Upon tempering at 500°C for up to 100 hours β_{Nb} precipitated in the matrix at martensitic α' needle boundaries, and at the twin boundaries. At higher tempering temperatures and after longer periods Nb-rich β_{Zr} also precipitated and coalesced. The oxidation rate was found to change with tempering time and temperature. The oxidation resistance of specimens tempered at 500°C for up to 100 hours was found to be higher than that of the as-quenched specimens. However, specimens tempered at 550°C for 1000 hours or at 600°C oxidized at a higher rate. This increase in rate has been attributed to formation of Nb-containing oxides on the coalesced Nb-rich precipitates, creation of weak oxide boundary zones, and localized failure in the oxide film.

INTRODUCTION

Zirconium-base alloys have found applications in the nuclear industry as a result of having the desired combination of mechanical properties and neutron absorption cross-section. Among these alloys, Zr-2.5wt%Nb has been used for pressure tubes and other reactor components. Since the properties of zirconium alloys in general can be controlled by heat treatments there have been many studies about phase transformations in the Zr-Nb system.[1-5] The heat treatment that has been used for strengthening Zr-2.5wt%Nb involves quenching from the β-phase field followed by tempering. (See Figure 1.)[6] The microstructural changes produced by this heat treatment have been investigated by many workers.[7-9] They observed that upon tempering, precipitation of a second phase took place in the matrix, at the martensite grain boundaries and at twin boundaries. The nature and composition of the precipitates were reported to vary with the tempering conditions.

A number of studies on the influence of heat treatment of Zr-2.5wt%Nb on aqueous corrosion and gaseous oxidation have revealed that annealing in the (α + β) phase region, annealing in the β-phase region, slow cooling through the (α + β) phase region and just quenching of the alloy decrease the corrosion resistance of the alloy.[10-15] Cox[16] and Cowgill and Smeltzer[17] reported slight improvements in the oxidation resistance upon annealing in the (α + β) phase field as compared to quenching from the β-phase. A heat treatment sequence consisting of quenching from the β-phase followed by a 24-hour anneal at 500°C has been reported to be ideal in terms of corrosion resistance.[18] Quenching from the (α + β) phase region followed by tempering at 550°C with or without intermediate cold work has also been reported to render microstructures most resistant to corrosion.[19] In some other investigations, changes in corrosion resistance of the Zr-2.5wt%Nb alloy with tempering conditions have also been reported.[11,18,20] This study, which forms part of an ongoing program of investigation of the oxidation/corrosion behavior of Zr-base alloys, was undertaken to extend the work of previous researchers and to clarify the influence of tempering temperature and time on the microstructure and consequently on the oxidation behavior of commercial-grade Zr-2.5wt%Nb.

MATERIALS AND PROCEDURES

Commercial-grade Zr-2.5wt%Nb alloy sheet containing ~1100 ppm oxygen was cut to give specimens 5 by 5 by 2 mm. These specimens were sealed in evacuated quartz capsules, given a solution treatment at 950°C for 30 minutes in the β-phase and quenched into water. The specimens were subsequently resealed in evacuated quartz capsules, tempered in a furnace with close temperature control at 500, 550, and 600°C for 10, 100, and 1000 hours, and again quenched. All the specimens, for optical microscopic examination as well as for oxidation measurements, were prepared under identical conditions to minimize the influence of surface preparation. Standard metallographic techniques followed by a final chemical polish-etch in a 10% HF, 25% H_2SO_4, 30% HNO_3 and balance water solution were used. Specimens for transmission electron microscopic (TEM) investigations were chemically polished in the above solution, disks 3 mm in diameter were punched out and electrolytically thinned to perforation at −20°C in a 10% perchloric acid, 90% ethanol solution.

Isothermal oxidation measurements on the different tempered specimens were carried out with a thermogravimetric analyzer at

☆ Submitted for publication March 1988; revised September 1988.

* Instituto de Pesquisas Energeticas e Nucleares, C.P. 11049 Cidade Universitaria, 05508 Sao Paulo, Brazil.

0010-9312/89/000133/$3.00/0

1989, National Association of Corrosion Engineers

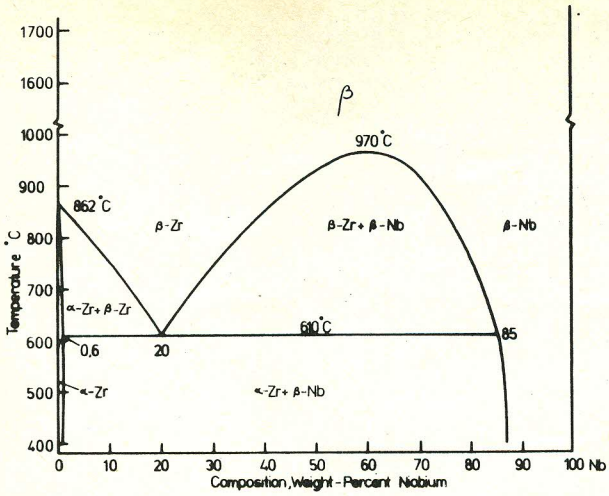

FIGURE 1. *Equilibrium phase diagram of the zirconium-niobium alloy system.*

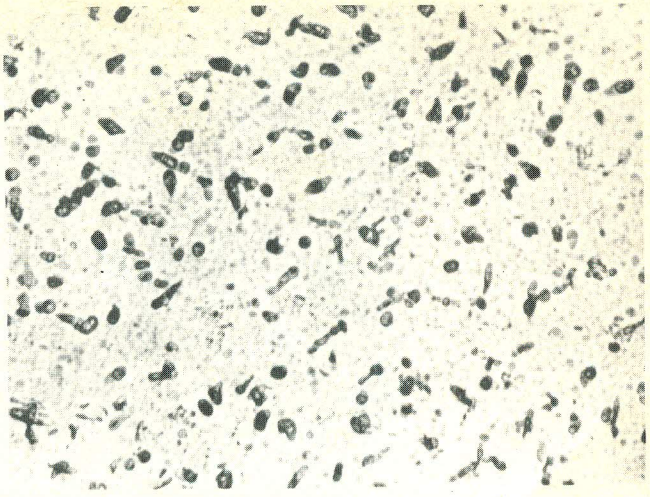

FIGURE 3. *Optical micrograph of Zr-2.5wt%Nb alloy tempered at 500°C for 1000 hours (400X).*

FIGURE 2. *Optical micrograph of Zr-2.5wt%Nb alloy tempered at 500°C for 10 hours (400X).*

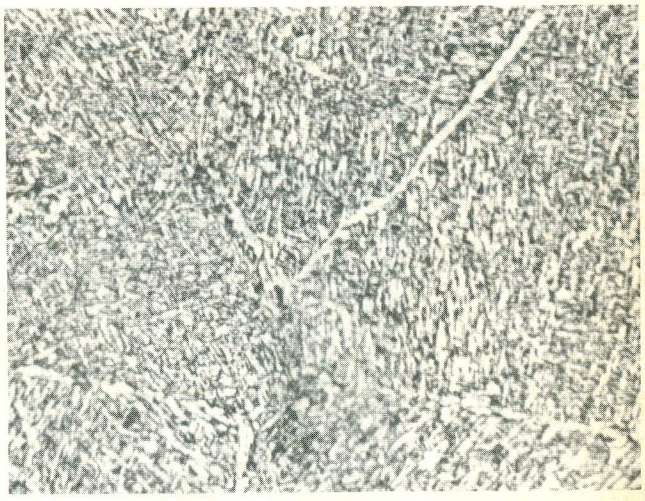

FIGURE 4. *Optical micrograph of Zr-2.5wt%Nb alloy tempered at 550°C for 1000 hours (400X).*

600°C for 400 minutes. The measurements were carried out in triplicate. The scatter in the oxidation data for specimens heat treated in the same batch was very small. The oxidized specimen surfaces were subsequently examined in a scanning electron microscope.

RESULTS AND DISCUSSION

Optical Microscopic Observations

The structure of the specimen tempered at 500°C for 10 hours revealed both rounded and slightly elongated precipitates in a martensitic matrix of α' as shown in Figure 2. The precipitates increased in size but decreased in number with increasing tempering time and were found to be β_{Nb} (determined by selected area diffraction [SAD] in the TEM) (see Figure 3). Tempering at 550°C for 10 hours resulted in a structure revealing fewer but larger precipitates in the matrix. Prolonged tempering at 550°C resulted in a structure shown in Figure 4, consisting of a light etching phase distributed in a Widmanstatten pattern in a matrix of the darker etching β_{Zr} phase. Tempering at 600°C for 10 hours produced coarsening of the matrix and coalescing of the precipitates. After 1000 hours at 600°C, a Widmanstatten structure shown in Figure 5 was produced that is typical of a specimen slowly cooled through the (α + β) phase field.

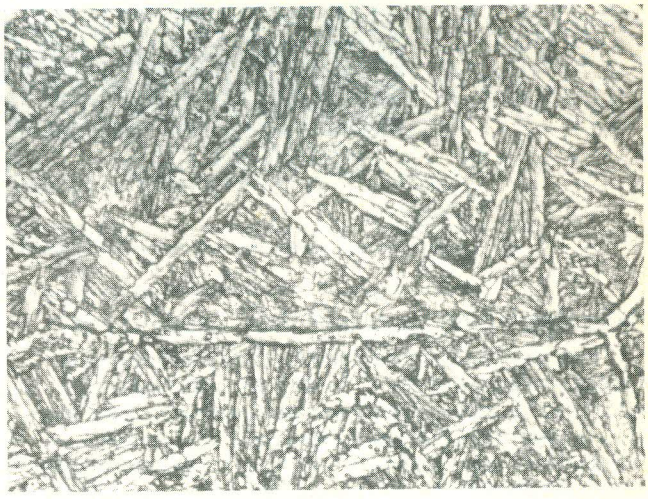

FIGURE 5. *Optical micrograph of Zr-2.5wt%Nb alloy tempered at 600°C for 1000 hours (400X).*

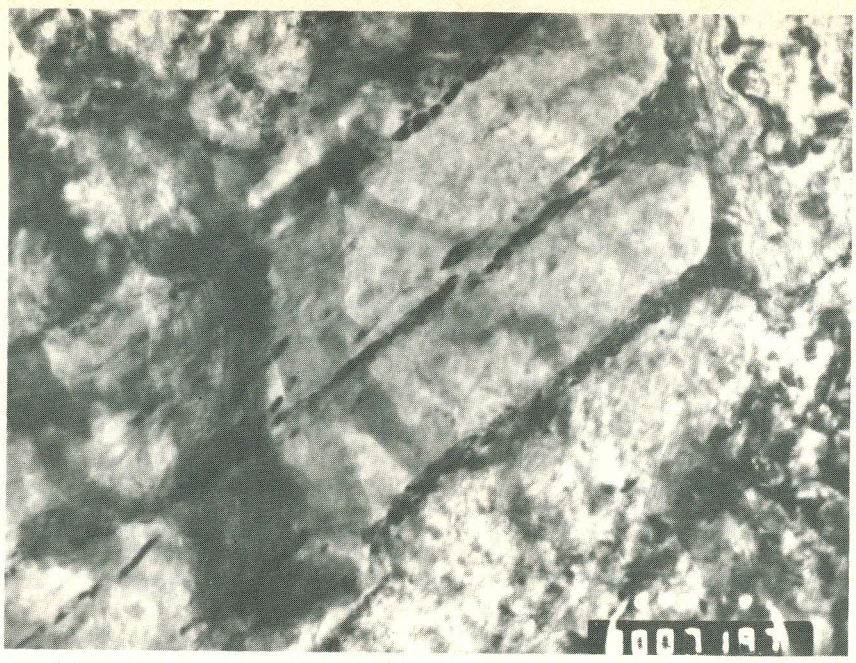

FIGURE 6. *Transmission electron micrograph of Zr-2.5wt%Nb alloy tempered at 500°C for 10 hours (80,000X).*

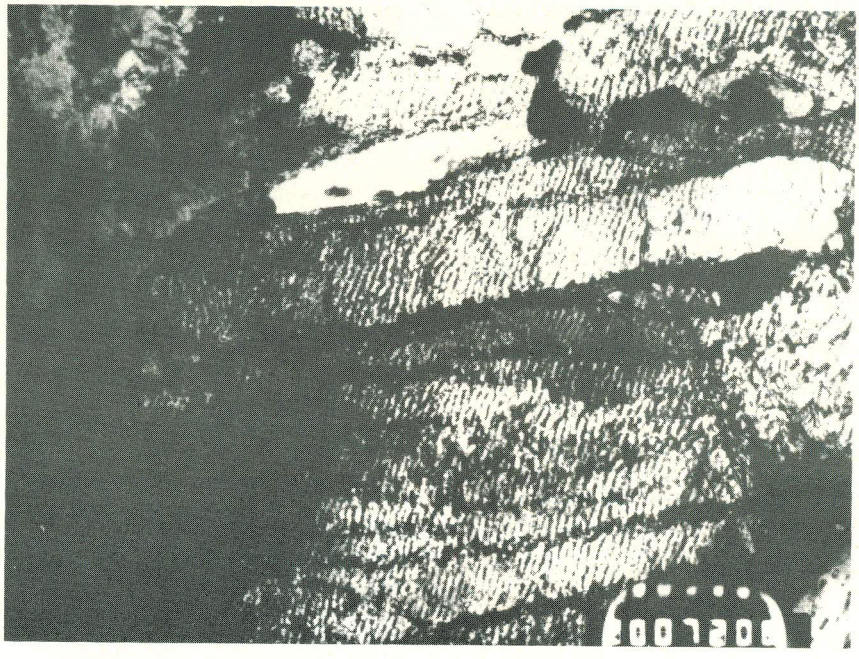

FIGURE 7. *Transmission electron micrograph of Zr-2.5wt%Nb alloy tempered at 500°C for 1000 hours (30,000X).*

Transmission Electron Microscopic Observations

The β-quenched specimen structure was characterized by internally twinned martensitic α′-needles. Upon tempering at 500°C for 10 hours the structure revealed precipitates at the α′-needle boundaries (see Figure 6) at microtwin boundaries and associated with matrix dislocations. In the specimen tempered at 500°C for 1000 hours, besides the gross rounded precipitates at the boundaries, very fine precipitates aligned within the matrix were also observed as shown in Figure 7. In specimens tempered at 550 and 600°C, the average precipitate size increased and they were present predominantly at α′-needle boundaries. A large number of aligned precipitates at pre-existing twin boundaries was also observed as shown in Figure 8 and found by SAD analysis to be Nb-rich β_{Zr}. Similar observations have been reported by Banerjee et al.[9] Prolonged tempering at 550 and 600°C leads to polygonization and growth of transformed β_{Zr}. The transformation of α′ to α and the coalescing of the β_{Zr} precipitates occurs to the extent that α has been seen to exist in a matrix of β_{Zr} as shown in Figure 9. Overall, with increasing tempering temperature and time, a change in the nature and composition of the precipitate has been observed as summarized in Table 1.

FIGURE 8. *Transmission electron micrograph of Zr-2.5wt%Nb alloy tempered at 600°C for 100 hours (9000X).*

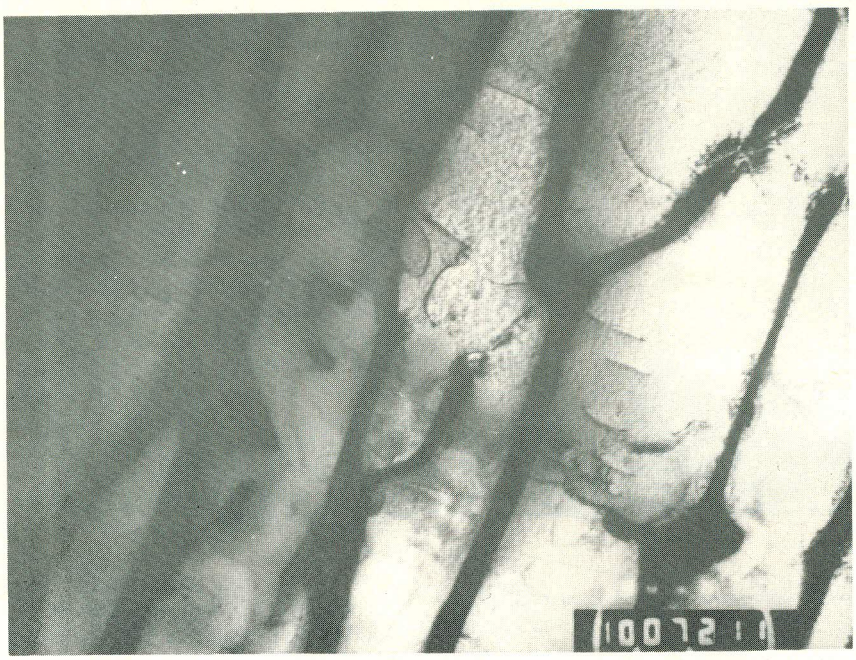

FIGURE 9. *Transmission electron micrograph of Zr-2.5wt%Nb alloy tempered at 600°C for 1000 hours (15,000X).*

TABLE 1
Phases and Precipitates Present in Tempered Zr-2.5wt%Nb Alloy

Tempering Time (h)	Tempering Temperature (°C)		
	500	550	600
10	$\alpha' + \beta_{Nb}$	$\alpha' + \beta_{Nb} + \beta_{Zr}$	$\alpha' + \beta_{Nb} + \beta_{Zr}$
100	$\alpha' + \beta_{Nb}$	$\alpha + \beta_{Zr}$	$\alpha + \beta_{Zr}$
1000	$\alpha' + \beta_{Nb} + \beta_{Zr}$	$\alpha + \beta_{Zr}$	$\alpha + \beta_{Zr}$

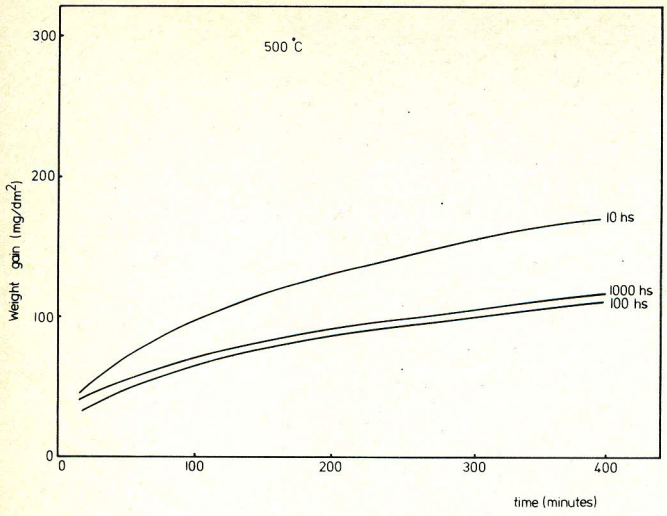

a

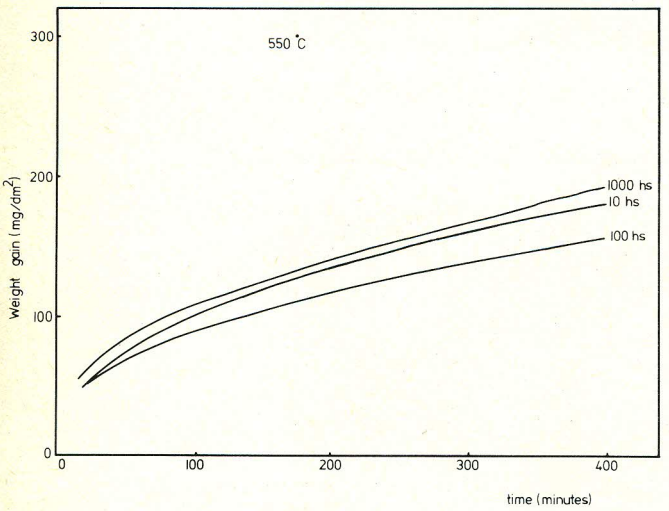

b

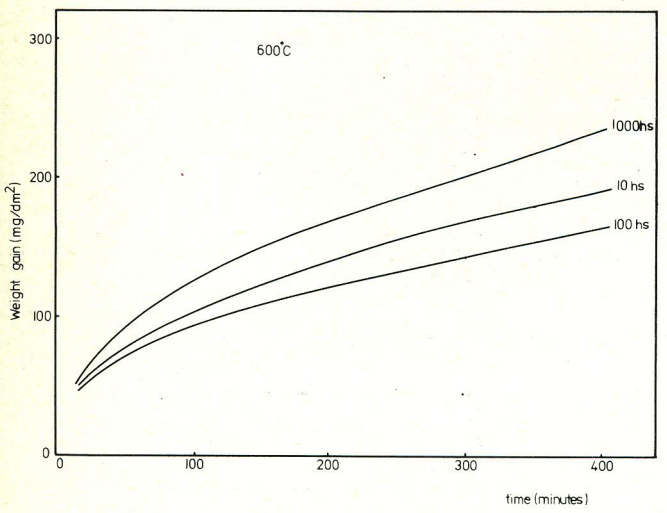

c

FIGURE 10. *Isothermal weight-gain versus time curves at 600°C in O_2 for Zr-2.5wt%Nb alloy tempered at (a) 500°C , (b) 550°C, and (c) 600°C.*

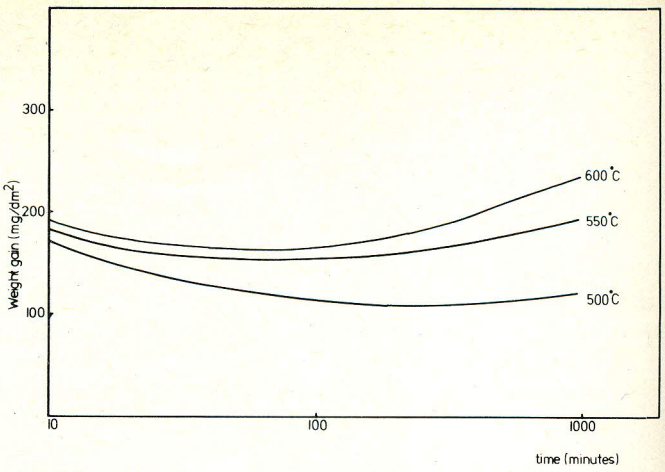

FIGURE 11. *Weight-gain of tempered Zr-2.5wt%Nb alloy at 600°C over 400 minutes vs tempering time.*

Oxidation Measurements

Figures 10 and 11 summarize the results of the isothermal oxidation measurements carried out at 600°C with the tempered specimens. The extent of oxidation of specimens tempered at 500°C for 10 hours is higher than that of specimens tempered for 1000 hours, which in turn is higher than that of the specimens tempered for 100 hours. This behavior can be attributed to the higher α' content in specimens tempered for 10 hours as compared to those tempered for longer times. The α' content leads to higher oxidation rate because of the higher Nb content of α'. Similar observations were made by Cowgill and Smeltzer.[17] Also, tempering at 500°C results in an even distribution of fine precipitates, which reduces the extent of oxidation. The oxidation behavior of specimens tempered at 550 and 600°C is different. The specimens tempered for 1000 hours oxidize faster than those tempered for 10 or 100 hours. This change in oxidation behavior upon increasing the tempering temperature is due to both the formation of large coalesced precipitates and oxide cracking. The coalesced precipitates oxidize at higher rates than martensitic α' or α-Zr. Morphological examinations of oxidized specimen surfaces have revealed regions with thicker oxide and cracks at the thick oxide/thin oxide boundary. The formation of similar thick oxide spots on β_{Nb} precipitates after prolonged oxidation of Zr-2.5wt%Nb have been reported and were attributed to the probable transfer of Nb from the precipitate to the oxide and its subsequent stoichiometric change to cause a volume increase. In this investigation thick oxide regions were observed after shorter times because of the higher oxidation temperature. X-ray diffractometry of the stripped oxide did not reveal Nb, its content being probably below the detection limit of the apparatus. Cowgill and Smeltzer[17] have reported the formation of thick oxides on α-phases and cracks in the oxide at the α/α' interface. Similar cracks in the oxide have been observed on specimens tempered at both 550 and 600°C for 1000 hours. (See Figure 12)

Comparison of the oxidation behavior of specimens tempered at all three temperatures reveals that the extent of oxidation increases with increasing tempering temperature and is attributable to increased precipitation kinetics. specimens tempered for 10 hours oxidize faster than those tempered for 100 hours at the same temperature. Similar observations were made by Cox,[20] who found the oxidation rate of Zr-2.5wt%Nb at 300°C in moist air to decrease with increase in tempering time up to 168 hours at 500°C. The higher oxidation resistance of specimens tempered for 100 hours at all three temperatures as compared to those tempered for 10 hours is due to the higher α' content in the latter and the even distribution of fine precipitates in the former. A fine pre-

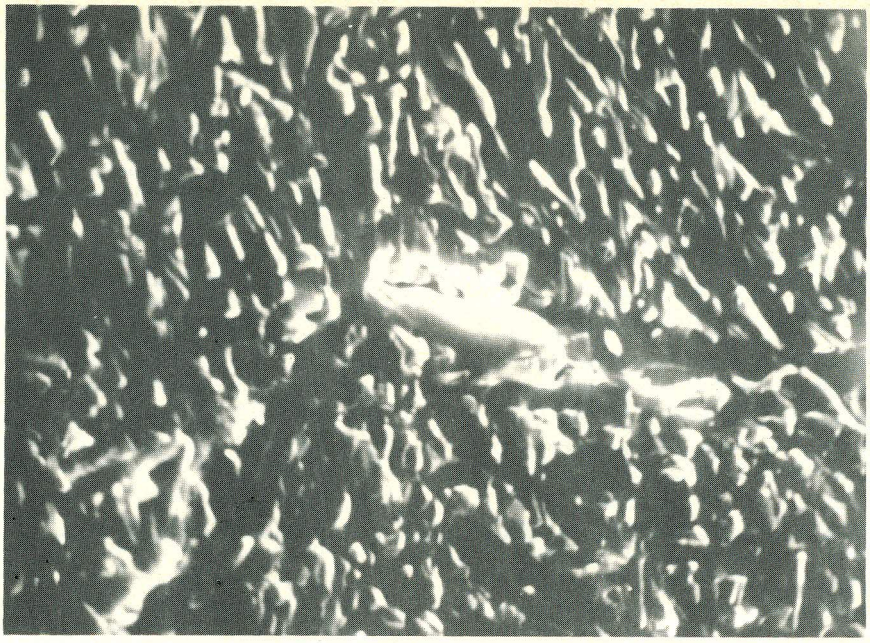

a

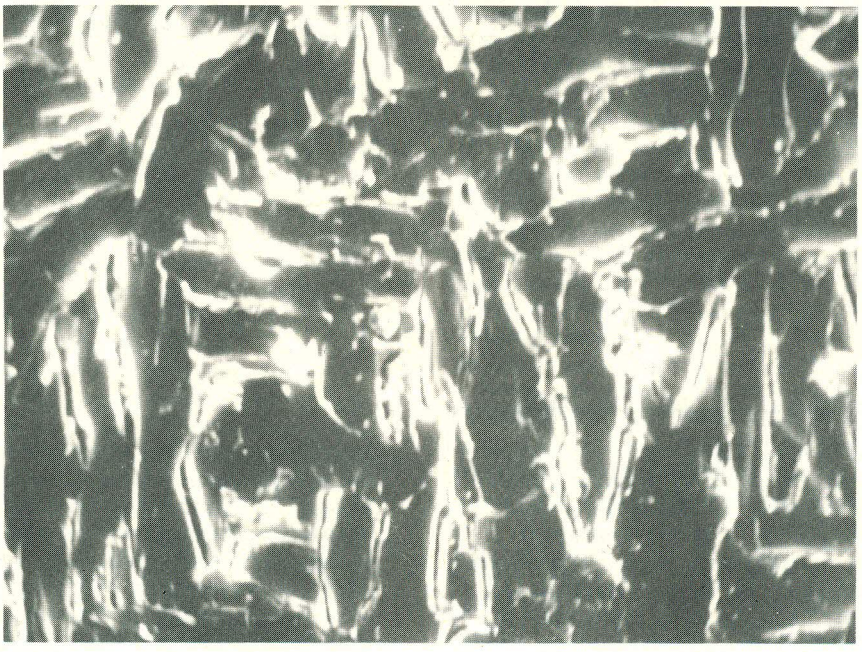

b

FIGURE 12. *Scanning electron micrographs of oxide surface on Zr-2.5wt%Nb alloy tempered at (a) 550°C for 1000 hours (3000X) and (b) 600°C for 1000 hours (2700X).*

cipitate size and even distribution is thought to permit strain accommodation between the oxide formed on the precipitate and that formed on the other areas.

CONCLUSIONS

▶ During the tempering of β-quenched Zr-2.5wt%Nb alloy, precipitation of second-phase particles takes place. Upon tempering at 500°C, depending on the duration, precipitation of β_{Nb} occurs in the matrix, at α′ grain boundaries, and at twin boundaries.

▶ After longer tempering times and higher tempering temperatures, β_{Zr} precipitates preferentially, the precipitates tend to coalesce, and α′ transforms to α.

▶ The oxidation behavior of the tempered alloy is influenced by the nature, distribution, and size of the precipitates.

▶ The oxidation resistance of specimens tempered for 100 hours can be attributed to a lower α′ content (as compared to those tempered for 10 hours) and even distribution of fine precipitates.

▶ Specimens tempered at 550°C and 600°C oxidized to a greater extent. This is considered to be due to the large coalesced precipitates.

▶ The decrease in oxidation resistance of specimens with coalesced precipitates is due to formation of niobium oxides on the niobium-rich precipitates, subsequent mismatch and cracking at the dissimilar oxide boundary, and localized failure of the oxide layer.

REFERENCES

1. D.L. Douglas, Atomic Energy Review, Supplement 1971 (Vienna, Austria: International Atomic Energy Agency (IAEA), 1971).
2. C.E.L. Hunt and P. Niessen, Journal of Nuclear Materials 38(1971): p. 17.
3. D.O. Northwood and D.T. Lim, Canadian Metallurgical Quarterly 18,21(1979): p. 441.
4. S. A-Aldridge and B-A. Cheadle, Journal of Nuclear Materials 42(1972): p. 32.
5. V.N. Shemyakin and G.D.Bainova, Fiz. Met. Metalloved 60,4(1985): p. 827.
6. C.E. Lundin and R.H. Cox, Proc. USAEC Symp. Zr. Alloy Develop, held Nov. 1962, GEAP-4089, vol. 1, 9.1, 1962.
7. C.D. Williams and R.W. Gilbert, Journal of Nuclear Materials 18(1966): p. 161.
8. G.P. Sabol, Journal of Nuclear Materials 34(1970): p. 142.
9. S. Banerjee, S.J. Vijaykumar and R. Krishnan, Journal of Nuclear Materials 62(1976): p. 229.
10. B. Cox, Advances in Corrosion Science and Technology, vol. 5, ed. M.G. Fontana and R.M. Staehle (New York, NY: Plenum Press 1976), p.173.
11. K. Anderko, W. Jung-Konig, H. Richter, H.W. Schleicher and U. Zweiker, Zeitschrift fur Metallkunde 53(1962): p. 503.
12. H.H. Klepfer, Journal of Nuclear Materials 9(1963): p. 65.
13. J.E. Lesurf, The Corrosion Behavior of 2.5%Nb Zirconium Alloy, Proc. ASTM Symp. Applications-Related Phenomena in Zr and its Alloys, ASTM-STP 458 (Philadelphia, PA: ASTM, 1968).
14. B.G. Parfenov, V.V. Gerasimov and G.I. Venediktova, Corrosion of Zirconium and Zirconium Alloys, Israel Program for Scientific Translations, Jerusalem, 34, 1969.
15. D.G. Lees, Corrosion Science 5(1965): p. 565.
16. B. Cox, Long-term Oxidation of Zr-2.5wt%Nb Alloy, AECL-5610, Chalk River Nuclear Laboratories, Chalk River, Ontario, Canada, 1976.
17. M.G. Cowgill and W.W. Smeltzer, Journal of Electrochemical Soc. 114(1967): p. 11.
18. S.B. Dalgaard, Corrosion of Reactor Materials, Vol. 2, IAEA Conference (Vienna, Austria: IAEA, 1962), p. 159.
19. E.N. Evans and D.G. Lees, U.K. Patent 988069, 1963.
20. B.Cox and J.A. Read, UKAEA Report AERE-r 4459, 1963.

Environmentally Assisted Cracking of Types 304L/316L/316NG Stainless Steel in 288°C Water ☆

*P.L. Andresen and C.L. Briant**

ABSTRACT

The objective of this study is to identity the causes of intergranular environmentally assisted cracking in non-chromium-depleted stainless steels, a phenomenon that has been observed under irradiated and unirradiated conditions. Special emphasis is placed on quantifying the possible effects of sulfur, phosphorus, and nitrogen relative to the effects of chromium depletion and aqueous impurities in altering both the crack-growth rate and cracking morphology in 288°C water.

Eleven custom and three commercial heats have been examined, including several containing exceptionally high sulfur levels. Slow strain rate (SSR) tests on smooth, cylindrical specimens and fracture mechanics, crack-growth rate tests on 1-T compact-type (CT) specimens were performed in 288°C water. The resulting cracking morphology and crack-growth rate data were interpreted using grain-boundary characterization data obtained by Auger electron spectroscopy and analytical electron microscopy.

In both SSR and CT tests, the amount of intergranular cracking correlated well only with grain-boundary sulfur segregation and not with phosphorus and nitrogen segregation; however, in no instance was a statistically significant enhancement in crack-growth rate observed in the fracture mechanics specimens. The ability of sulfur to produce intergranular cracking was much greater in the SSR tests in the potentiostatically controlled, 2.5 pH H_2SO_4 than in SSR or CT tests in pure water. Chromium depletion and/or aqueous impurities can have a much more pronounced effect on crack-growth rates in stainless steels than grain-boundary segregants. However, effects of these and other segregants cannot be precluded since, for example: (1) even small changes in crack-growth rate can be significant in terms of component lifetime; (2) their role may be more important for very short cracks in the early stages of cracking, where the crack-tip corrosion potential in oxygen-containing solutions is much more oxidizing than for long cracks; and (3) despite the use of very high sulfur levels in this study, the impurity profiles near grain boundaries resulting from irradiation-induced segregation may lead to vastly more impurity in the vicinity of the grain boundary.

INTRODUCTION

Over the past two decades environmental cracking of austenitic stainless steels in high-temperature water has been the subject of widespread research, primarily as a result of incidents of intergranular stress corrosion cracking in light water reactors.[1-4] Cracking was initially attributed to grain-boundary chromium depletion, which occurs as chromium carbides nucleate and grow in the grain boundaries. As the carbides grow, the carbon rapidly diffuses to the carbide/matrix interface and is available to the growing carbide. Since chromium diffuses much more slowly, it is drawn from the surrounding material, which then becomes

☆ Submitted for publication March 1988.

* Corporate Research and Development Center, General Electric Company, 1 River Road K1-3A43, Schenectady, NY 12301.

0010-9312/89/000135/$3.00/0

© 1989, National Association of Corrosion Engineers